Available online at www.sciencedirect.com

ScienceDirect

Mendeleev Commun., 2023, **33**, 124–126

Mendeleev Communications

Synthesis of ceria nanosheets on the surface of $Ce(NO_3)_3$ solution by interaction with gaseous ammonia

Larisa B. Gulina,* Polina O. Skripnyak and Valeri P. Tolstoy

Institute of Chemistry, St. Petersburg State University, 199034 St. Petersburg, Russian Federation. E-mail: l.gulina@spbu.ru

DOI: 10.1016/j.mencom.2023.01.039

The surfactant-free synthesis of a solid film of ceria was carried out at the air–water interface from an aqueous solution of $Ce(NO_3)_3$ and gaseous NH_3 as reactants. The synthesized $CeO_{2-x}\cdot n\,H_2O$ film consists of 2D nanocrystals with a fluorite structure. The film can form a planar coating on the surface of a solid substrate or transform into curved fragments upon drying, depending on the synthesis conditions.

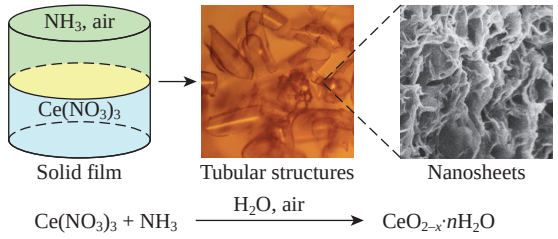

Keywords: ceria, nanocrystals, films, interface, hydrolysis.

Ceria-based materials are widely used in the design of catalysts,[1,2] sensors,[3] solid electrolytes,[4] electrochromic and protective coatings,[5] electrorheological liquids,[6] as well as in bioactive and medical applications.[7–9] The nanoscale effect is observed during the transition from the bulk to the nanocrystalline state; therefore, the properties of ceria depend on the particle size. It has been noted[10,11] that the activity in redox processes is affected not only by the size, but also by the morphology of nanocrystalline CeO_2 particles. It is known[12] that with a decrease in the size of ceria particles, the fraction of Ce^{3+} in their composition increases.

It is possible to obtain CeO_2 nanocrystals by precipitation reactions in solutions,[13–16] including the use of hydrothermal and high-temperature treatment.[17,18] Synthesis at the interface has some advantages over precipitation in the bulk of a homogeneous solution.[19] The main one is the limited zone of interaction between the reactants, which provides nanoscale characteristics of the reaction products and limits the aggregation of the resulting nanoparticles.

The formation of a film of insoluble compounds at the interface between two immiscible liquids can be accompanied by self-assembly, coagulation and polymerization reactions.[20] Under such conditions, organometallic compounds or hybrid organic–inorganic particles were obtained.[21] Features of the solution–gas interface are widely used in the preparation of films by the Langmuir–Blodgett technology using the self-assembly of amphiphilic molecules.[22,23] However, when a surfactant is added, two interfaces are formed: solution–surfactant and surfactant–air. Unlike the methods mentioned above, gas–solution interface synthesis (GSIT)[24–27] does not use surfactants to create a solid film on the solution surface. Instead, GSIT is based on the interaction between a salt solution and a gaseous reagent at a planar interface. Previously, it was found that silver nanoparticles,[28] films of oxides,[29] halides[30] and chalcogenides[31,32] of metals, as well as gradient films of various inorganic compounds, capable of transforming into microscrolls upon drying,[24–27] can be obtained under such conditions.

In this work, a nanostructured film and particles of $CeO_{2-x}\cdot n\,H_2O$ were synthesized† by the GSIT method due to the interaction between an aqueous solution of $Ce(NO_3)_3$ and NH_3 from the gas phase at a planar interface.

The reactions of hydrolysis [reaction (1)] and oxidation in air [reaction (2)] can occur on the surface of an aqueous solution of cerium nitrate under the action of gaseous ammonia:

$$Ce(NO_3)_3 + 3H_2O + 3NH_3 \rightarrow Ce(OH)_3 + 3NH_4NO_3, \quad (1)$$

$$4Ce(OH)_3 + O_2 \rightarrow 4CeO_2 + 6H_2O. \quad (2)$$

The removal of water-soluble reaction products occurs when the resulting transparent free-floating film is kept on the surface of distilled water. Next, the film is transferred to the surface of a solid substrate and dried in air at room temperature. The reaction product can contain both Ce^{3+} and Ce^{4+} ions, as well as a significant amount of water molecules in the composition, so its formula corresponds to the non-stoichiometric compound $CeO_{2-x}\cdot n\,H_2O$.

Figure 1 shows optical micrographs‡ of the reaction products obtained on the surface of $Ce(NO_3)_3$ solutions with a concentration of 0.02 M [Figure 1(*a*)–(*c*)] and 0.04 M [Figure 1(*d*)] for 3–12 min of interaction. It can be noted that when using a solution with a lower concentration, a film is formed that has pores and cracks at

† $Ce(NO_3)_3$ (analytical grade, Vekton) and $NH_3\cdot H_2O$ (high purity grade, Vekton) were used as reagents. Aqueous solutions were prepared using high-purity Milli-Q water with a resistivity of more than 18 MΩ cm^{-1}. The synthesis procedure is similar to that described earlier.[26,29] Briefly, a container with a dilute (1 : 1) ammonia solution (2 ml), which served as the source of the gaseous reagent, was placed in a 50 ml glass-line closed reactor. Then a flat vessel with $Ce(NO_3)_3$ solution (5 ml) was placed next to the container with $NH_3\cdot H_2O$. The surface areas of the reagent solutions were 4 and 2 cm^2, respectively. The synthesis was carried out under stationary conditions at room temperature and atmospheric pressure. A transparent film formed on the surface of the salt solution within 3–20 min. Then the film was transferred to the surface of distilled water (500 ml) and washed for 20 min. Afterwards, the film was placed on the surface of glass or single-crystal silicon and dried at room temperature.

‡ The as-prepared samples were examined using optical microscopy, scanning electron microscopy (SEM), X-ray diffraction (XRD) analysis and energy-dispersive X-ray (EDX) microanalysis. Morphology was investigated using a Micromed optical microscope with a magnification of 40–1000×, a Zeiss EVO-40EP scanning electron microscope equipped with an Oxford Instruments INCA 350 EDX analyzer or a Zeiss Supra-40VP scanning electron microscope. XRD analysis was performed on a Bruker D2 Phaser diffractometer equipped with a CuKα X-ray source (λ = 1.5406 Å).

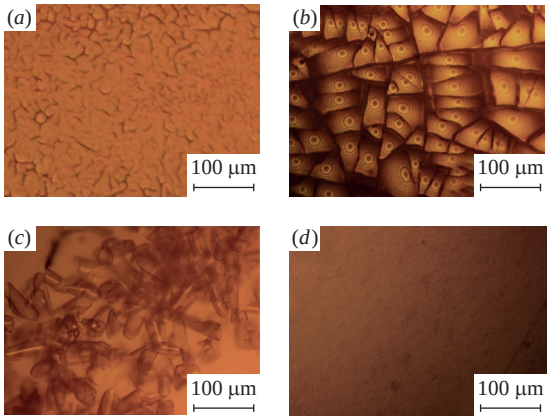

Figure 1 Optical micrographs of reaction products prepared on the surface of (*a*)–(*c*) 0.02 M and (*d*) 0.04 M solutions of $Ce(NO_3)_3$ for (*a*) 3, (*b*) 6 and (*c*),(*d*) 12 min of interaction with gaseous NH_3 after washing and transfer to a glass support.

the initial stage, as can be seen from Figure 1(*a*). The film obtained as a result of the 6-min interaction, during drying, is divided into separate fragments with a certain radius of curvature. This is evidenced by the interference pattern with numerous Newton rings [Figure 1(*b*)]. Drying of the film obtained within 12 min of interaction leads to the formation of tubular structures [Figure 1(*c*)]. When using a more concentrated solution, such a film is formed in the very first minutes and, upon drying, retains a planar geometry [see Figure 1(*d*)]. There were no significant changes in its morphology with an increase in the synthesis time.

The results of the SEM study of the synthesized tubular structures are shown in Figure 2. One can see a general view of the tubular structures of the film up to 2 μm thick [Figure 2(*a*)]. Figure 2(*b*) shows a side view of the wall of the tubular structure, revealing that the film is composed of nanosheets about 20 nm thick. It can be seen that the nanosheets have a predominant orientation. According to EDX microanalysis data, the synthesized films and particles contain only Ce and O atoms, which confirms the formula of the synthesized non-stoichiometric compound $CeO_{2-x} \cdot n\,H_2O$.

Powder XRD patterns of the tubular structures and the film on the silicon surface are shown in Figure 3. A series of diffraction peaks at 2θ of 28.7°, 32.8°, 47.4°, 56.3° and others corresponds to the *fcc* crystal structure of fluorite.[33] The sharper maxima in the X-ray diffraction pattern of the curved particles indicate that they are better crystallized than the film containing an amorphous component.

According to the experimental results, the following model of film formation at the interface can be proposed. At the initial moment, a discontinuous film of cerium(III) hydroxide is formed on the surface of a solution with a lower concentration according to

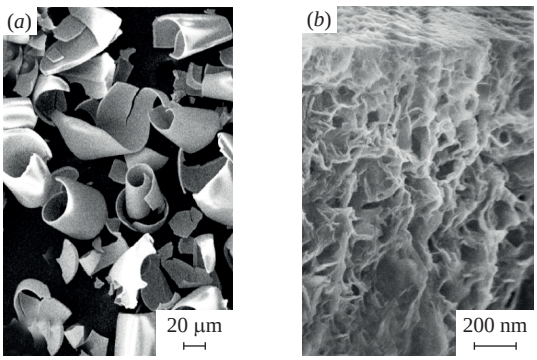

Figure 2 SEM images of the reaction products prepared on the surface of a 0.02 M $Ce(NO_3)_3$ solution during 12 min of interaction with gaseous NH_3 after washing and transfer on a silicon support: (*a*) general view and (*b*) cross-section view.

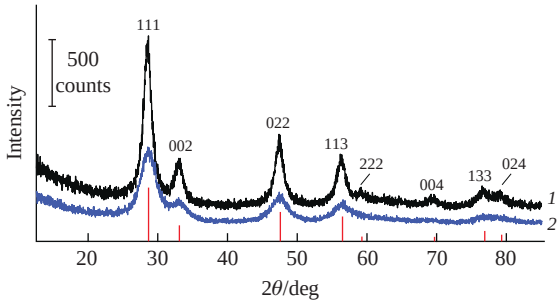

Figure 3 XRD patterns of (*1*) tubular structures and (*2*) the film of synthesized $CeO_{2-x} \cdot n\,H_2O$.

reaction (1). Further, the interaction continues in depth, since the gaseous reagent can penetrate through the pores. In this case, $CeO_{2-x} \cdot n\,H_2O$ nanosheets with the fluorite crystal structure are formed. The direction of crystal growth, perpendicular to the phase boundary, determines the predominant orientation of the nanosheets. Thus, a gradient of crystal packing density is formed over the film thickness. When the interaction time is longer, the gradient film becomes thicker, and the difference in the density of its sides also increases. The film density gradient is visible on the SEM image [see Figure 2(*b*)]. During the drying of this gradient film, due to uneven removal of water, mechanical forces arise that contribute to the separation of the film into curved fragments. Thus, the radius of curvature of the pieces depends on the density and humidity gradients in the synthesized film. As for the formation of $CeO_{2-x} \cdot n H_2O$ on the surface of a more concentrated solution, the rapid formation of a solid film does not allow the development of a density gradient over the thickness. Therefore, this film retains its planar geometry when dry.

In conclusion, a $CeO_{2-x} \cdot n\,H_2O$ film can be synthesized at the gas–solution interface by an reacting an aqueous solution of $Ce(NO_3)_3$ with gaseous NH_3. The film consists of 2D nanocrystals with a fluorite structure. The concentration of the solution determines the morphology of the reaction product. For example, on the surface of a 0.04 M cerium salt solution, a flat homogeneous film can be obtained. In contrast, a gradient film formed on the surface of a 0.02 M solution is separated into fragments with a certain radius of curvature upon drying. The radius of curvature of the pieces in this case depends on the thickness of the film or, in other words, on the duration of the interaction.

We expect that the synthesized $CeO_{2-x} \cdot n\,H_2O$ films can be used to create protective or bioactive coatings. At the same time, tubular structures have a morphology that is promising for the design of new catalysts and sorbents.

This work was supported by the Russian Science Foundation (project no. 22-29-00687, https://www.rscf.ru/project/22-29-00687/). The XRD analysis was carried out at the X-Ray Diffraction Center of Saint-Petersburg State University. The SEM study was performed at the Nanotechnology Center of Saint-Petersburg State University.

References

1 T. Montini, M. Melchionna, M. Monai and P. Fornasiero, *Chem. Rev.*, 2016, **116**, 5987.
2 I. V. Zagaynov, A. S. Loktev, I. E. Mukhin, A. A. Konovalov and A. G. Dedov, *Mendeleev Commun.*, 2022, **32**, 129.
3 P. Jasinski, T. Suzuki and H. U. Anderson, *Sens. Actuators, B*, 2003, **95**, 73.
4 H. Inaba and H. Tagawa, *Solid State Ionics*, 1996, **83**, 1.
5 N. Özer, *Sol. Energy Mater. Sol. Cells*, 2001, **68**, 391.
6 A. V. Agafonov, A. S. Kraev, T. V. Gerasimova, O. L. Evdokimova, T. O. Shekunova, A. E. Baranchikov, L. P. Borilo, O. S. Ivanova, V. V. Kozik and V. K. Ivanov, *Russ. J. Inorg. Chem.*, 2017, **62**, 625 (*Zh. Neorg. Khim.*, 2017, **62**, 627).

7 I. V. Kolesnik, A. B. Shcherbakov, T. O. Kozlova, D. A. Kozlov and V. K. Ivanov, *Russ. J. Inorg. Chem.*, 2020, **65**, 960 (*Zh. Neorg. Khim.*, 2020, **65**, 872).
8 A. L. Popov, N. Popova, D. J. Gould, A. B. Shcherbakov, G. B. Sukhorukov and V. K. Ivanov, *ACS Appl. Mater. Interfaces*, 2018, **10**, 14367.
9 A. B. Shcherbakov, N. M. Zholobak, N. Ya. Spivak and V. K. Ivanov, *Russ. J. Inorg. Chem.*, 2014, **59**, 1556.
10 D. Zhang, X. Du, L. Shi and R. Gao, *Dalton Trans.*, 2012, **41**, 14455.
11 C. T. Campbell and C. H. F. Peden, *Science*, 2005, **309**, 713.
12 V. K. Ivanov, A. B. Shcherbakov and A. V. Usatenko, *Russ. Chem. Rev.*, 2009, **78**, 855 (*Usp. Khim.*, 2009, **78**, 924).
13 V. K. Ivanov, O. S. Polezhaeva and Yu. D. Tret'yakov, *Russ. J. Gen. Chem.*, 2010, **80**, 604 [*Ross. Khim. Zh.*, 2010, **53** (2), 56].
14 A. V. Agafonov, A. S. Krayev, O. I. Davydova, K. V. Ivanov, T. O. Shekunova, A. E. Baranchikov, O. S. Ivanova, L. P. Borilo, A. V. Garshev, V. V. Kozik and V. K. Ivanov, *RSC Adv.*, 2016, **6**, 88851.
15 V. K. Ivanov, O. S. Polezhaeva, G. P. Kopitsa, A. E. Baranchikov and Yu. D. Tret'yakov, *Inorg. Mater.*, 2008, **44**, 272 (*Neorg. Mater.*, 2008, **44**, 324).
16 P. A. Yurova, N. Yu. Tabachkova, I. A. Stenina and A. B. Yaroslavtsev, *J. Nanopart. Res.*, 2020, **22**, 318.
17 V. K. Ivanov, O. S. Polezhaeva, G. P. Kopitsa, P. P. Fedorov, K. Pranzas and V. V. Runov, *Russ. J. Inorg. Chem.*, 2009, **54**, 1689 (*Zh. Neorg. Khim.*, 2009, **54**, 1767).
18 E. Özkan, A. Hofmann, M. Votsmeier, W. Wang, X. Huang, C. Kübel, F. Badaczewski, K. Turke, S. Werner and B. M. Smarsly, *Langmuir*, 2021, **37**, 2563.
19 X. Wang, Q. Peng and Y. Li, *Acc. Chem. Res.*, 2007, **40**, 635.
20 C. N. R. Rao and K. P. Kalyanikutty, *Acc. Chem. Res.*, 2008, **41**, 489.
21 E. N. Golubina, N. F. Kizim, E. V. Sinyugina and I. N. Chernyshev, *Mendeleev Commun.*, 2018, **28**, 110.
22 N. S. Chirkov, A. V. Michailov, P. S. Vlasov and B. A. Noskov, *Mendeleev Commun.*, 2022, **32**, 192.
23 A. V. Kazak, M. A. Marchenkova, A. I. Smirnova, A. Yu. Seregin, A. V. Rogachev, J. Warias, B. Murphy, E. Yu. Tereschenko and N. V. Usol'tseva, *Mendeleev Commun.*, 2020, **30**, 52.
24 V. P. Tolstoi and L. B. Gulina, *Russ. J. Gen. Chem.*, 2013, **83**, 1635 (*Zh. Obshch. Khim.*, 2013, **83**, 1409).
25 L. B. Gulina and V. P. Tolstoy, *Russ. J. Gen. Chem.*, 2014, **84**, 1472 (*Zh. Obshch. Khim.*, 2014, **84**, 1243).
26 L. B. Gulina, V. P. Tolstoy, A. A. Solovev, V. E. Gurenko, G. Huang and Y. Mei, *Prog. Nat. Sci.: Mater. Int.*, 2020, **30**, 279.
27 V. V. Strykanova, L. B. Gulina, V. P. Tolstoy, E. V. Tolstobrov, D. V. Danilov and I. Skvortsova, *ACS Omega*, 2020, **5**, 15728.
28 L. B. Gulina, V. P. Tolstoy and E. V. Tolstobrov, *Mendeleev Commun.*, 2017, **27**, 634.
29 V. P. Tolstoy, L. B. Gulina, A. A. Golubeva, S. S. Ermakov, V. E. Gurenko, D. V. Navolotskaya, N. I. Vladimirova and A. V. Koroleva, *J. Solid State Electrochem.*, 2019, **23**, 573.
30 L. B. Gulina, V. P. Tolstoy, I. A. Kasatkin, I. E. Kolesnikov and D. V. Danilov, *J. Fluorine Chem.*, 2017, **200**, 18.
31 S. H. Pawar, P. N. Bhosale, M. D. Uplane and S. Tamhankar, *Thin Solid Films*, 1983, **110**, 165.
32 S. H. Pawar and P. N. Bhosale, *Mater. Chem. Phys.*, 1984, **11**, 461.
33 R. W. G. Wyckoff, *Crystal Structures*, 2nd edn., Interscience Publishers, New York, 1963, vol. 1, pp. 239–444.

Received: 14th July 2022; Com. 22/6958